SL-08-013

Transient Simulation of Airflow and Pollutant Dispersion Under Mixing Flow and Buoyancy Driven Flow Regimes in Residential Buildings

Donghyun Rim
Student Member ASHRAE

Atila Novoselac, PhD
Associate Member ASHRAE

ABSTRACT

The distribution of airflow in a residential building varies with the periodic operation of a heating, ventilating and air-conditioning (HVAC) system. Depending on the HVAC fan operation, mixing airflow (fan ON) or stratified airflow (fan OFF) occurs in the space. The objectives of this study are 1) to examine the time needed for room air to stabilize after a central ventilation fan turns ON/OFF and 2) to evaluate how the difference in distribution of gaseous and particulate pollutants in the space depends on fan operation mode. In the study, experiments measured the spatial distribution of airflow and pollutant concentrations in a full-scale environmental chamber. The measured data then provided the basis to establish a reliable computational fluid dynamics (CFD) model, which investigated the concentrations of gaseous and particulate pollutants depending on the mechanical fan operation mode. The results indicate that the transition between mixing flow and stratified flow occurs in a time scale of seconds, implying that the airflow in residential buildings is primarily mixing or stratified flow. The results show little spatial variation of tracer gas and particles in the mixing flow regime, whereas larger temporal and spatial variations are present in stratified flow. Additionally, the variations in particle concentrations are higher than those in gaseous concentrations. In certain areas of the room the particle concentration with stratified flow is up to thirty times higher than that with mixing flow, implying a high potential of exposure to particles when the fan is OFF.

INTRODUCTION

Thermal comfort and level of exposure to indoor pollutants vary with airflow pattern in an occupied space (Novoselac and Sebric 2002; Zhao et al. 2004; Bouilly 2005). In residential buildings, where periodic operation of air-conditioning systems occurs, the indoor airflow pattern mainly depends on the mechanical operation of the fan and the presence of heat sources. During fan operation, forced convection often dominates over the buoyant airflow generated by indoor heat sources, which creates a mixing flow regime in the space. However, when the fan is off, buoyant thermal plumes from indoor heat sources become dominant, causing buoyancy driven flow.

Given that the transport of indoor pollutants is directly related to the airflow distribution in the space (Lin et al. 2005; Gao and Liu 2007; Li et. al 2007), the mixing and buoyant airflows each have distinct effects on the transport of indoor airborne pollutants. With the mixing airflow, the large momentum of supply air scatters pollutants through the space, providing more or less uniform distribution of pollutants. Conversely, in a room with buoyancy driven airflow, the indoor heat sources raise the air to upper level of the space, causing thermal stratification and non-uniform pollutant concentrations in the space.

On average, residential buildings operate their HVAC fans 17% of the day (Ward et al. 2005). Consequently, both mixing airflow and buoyant airflow periodically exist in residential buildings. Previous studies have investigated how pollutants transport under mixing flow and buoyancy driven flow regimes. In these studies, researchers often used displacement ventilation to create buoyant airflow from indoor heat sources. Huang et al. (2004) conducted a numerical study of exposure to household contaminants, including carbon dioxide and carbon monoxide, in a single-family house with different airflow patterns. They reported lower occupant exposure with buoyant flow than with mixing flow. Lin et al. (2005) measured the concentrations of gaseous

Donghyun Rim is a doctoral student and **Atila Novoselac** is an assistant professor in the Department of Civil, Architectural and Environmental Engineering, The University of Texas at Austin, TX.

pollutants such as carbon monoxide and different VOCs with mixing and displacement ventilation in offices, industrial workshops, and public places. They concluded that the buoyant airflow associated with displacement ventilation provides better indoor air quality in the breathing zone than mixing ventilation. He et al. (2005) used a validated computer model to examine dispersion of a gaseous pollutant (SF_6) emitted from a floor surface and found that concentration stratification exists with displacement ventilation. Considering particles (1~10 μm) that enter the space with supply air (by infiltration or ventilation), Gao and Liu (2007) found lower exposure for occupants in the room with air mixing than in the room with buoyant flow. Taken together, these previous research results suggest that indoor airflow pattern and air mixing associated with operating ventilation fans could have significant impact on pollutant transport and occupant exposure in residential buildings.

The studies in literature extensively examined the airflow and pollutant concentration variations with airflow patterns. However, the previous studies all lack information on the transition period between the mixing flow regime and the buoyancy driven flow regime. The transition between mixing flow and buoyant flow occurs frequently in residential buildings since periodic operation of fan is common. In addition, the majority of previous studies focused on pollutant concentrations due to steady source emissions. However, transient pollutant transport, such as a short release of pollutant in an occupied space, may be the more common and relevant problem. Examples of transient contaminant release are combustion sources and particle re-suspension from surfaces created by different indoor activities.

The objectives of this study were as follows:

1. Examine the time needed for room airflow to stabilize after a central residential fan turns ON/OFF
2. Evaluate the effects of airflow distribution on spatial and temporal concentrations of gaseous and particulate pollutants emitted from a source which is active for a short-time period.

Experiments in a full scale environmental chamber were conducted to measure the airflow dynamics due to residential fan usage. The experiments were used to validate numerical simulations that determined the pollutant distribution in the space for different fan operations. The following sections will be presented in the following order: airflow dynamics with ventilation fan operation, experimental validation of numerical models for unsteady-state contaminant flow analysis, and prediction of pollutant distribution in a room using the validated numerical model.

AIRFLOW DYNAMICS WITH RESIDENTIAL FAN OPERATION

The first set of experiments measured air flow velocity magnitudes for two fan operation modes: fan ON and fan OFF. To analyze the transition of airflow from mixing flow to buoyancy driven flow and vice versa, an environmental chamber of volume 67 m^3 (2366 ft^3) with a thermal manikin was used. The environmental chamber was equipped with an air handling unit (AHU), which controlled and monitored the supply airflow rate, temperature and humidity of the air in the room. The manikin had an accurate geometrical similarity to a real person and the electric heaters inside the skin shell generated heat flux in each part of the body.

Experimental Setup

Figure 1 shows the experimental setup for monitoring air speed at characteristic points in the space with intermittent fan operation. The experimental setup in the environmental chamber represents a typical residential room. A thermal manikin which simulates a human presence was placed in the center of the chamber (Figure 1a). The manikin had a total heat flux of 90W across the skin and cloth surfaces. The convective portion of this flux created a buoyant thermal plume in the vicinity of the manikin. In addition, indoor heat sources, such as sun patches on the floor and heat sources such as TVs or

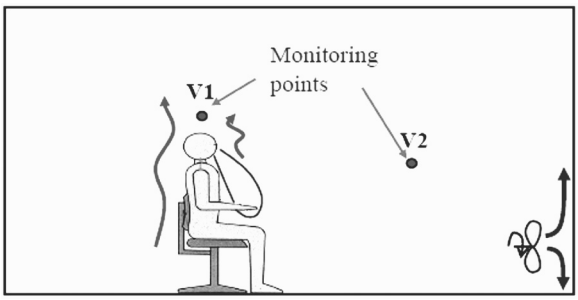

(a)

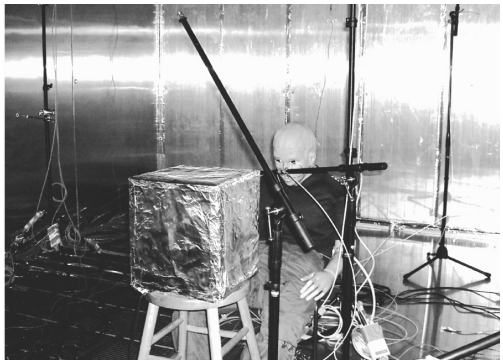

(b)

Figure 1 *Experimental setup for analyses of effects of fan operation, with (a) being a schematic diagram of experiment, and (b) being a manikan and velocity sensors.*

computers, were distributed in the chamber to simulate the environment typical for a residential space (Figure 1b).

To simulate a residential room when the mechanical ventilation is OFF and only infiltration is present, supply air was provided with low speed. In this case the airflow in the space was driven primarily by buoyancy from indoor heat sources. A mixing fan in the space was used to convert buoyant flow to mixing flow. The power and position of the fan were adjusted to generate forced convection typical for a residential space with the air-conditioning system working. The transition of the airflow field between buoyant flow and mixing flow and vice versa was analyzed by examining the transient air speed in the space for intermittent operation of the mixing fan.

Spatial distribution of air speed was measured using omni-directional low velocity sensors, which measure mean velocity magnitude. The airflow direction was determined using smoke visualization tests. The airflow data were collected at 16 positions in space. The analysis in this paper will focus on the two characteristic points: (1) the location 25 cm (9.8 in) above the manikin head (V1) and (2) the location in the stagnation zone in the room (V2), as shown in Figure 1a. The selection of the two monitoring points was based on a study by Murakami et al. (1997), which analyzed the boundary layer of the thermal plume around a human body. They found that in a room with still air the thermal boundary layer at foot level is about 5 cm (2.0 in) thick and around the neck 19 cm (7.7 in). In our experiment, the monitoring point in the stagnation zone (V2) was located at a distance of approximately 60cm (24 in) from the manikin.

Airflow intensity is the largest above the thermal manikin due to the effects of buoyant forces from the whole body. The air speed above the head (V1) represents the strength of the plume. On the other hand the air speed in the stagnation zone (V2) illustrates the effects of momentum forces induced by the fan. When the fan operates, the air velocities in the vicinity of chamber surfaces ranged from 0.5 - 2.5 m/s (1.6-8.2 ft/s), and the velocities in the central spaces were in the range 0.15-0.25 m/s (0.49-0.82 ft/s). To investigate the transition period from the buoyant airflow to the mixing flow, the fan operation was intermittent with several minutes of ON and OFF periods.

Room Airflow Dynamics with Intermittent Operation of Ventilation Fan

The experiments applied intermittent fan operation typical of residential air-conditioning systems. Figure 2 shows the velocity magnitudes at V1 (above the head) and at V2 (stagnation zone) for the two different fan operation modes. When the fan was OFF, the ambient airflow velocity at V2 (stagnation zone) does not fluctuate, indicating that the ambient airflow is not affected by the buoyant thermal plume. Also, the average velocity magnitudes at V1 (above the head) and at V2 (stagnation zone) are 0.19 m/s (0.62 ft/s) and 0.03 m/s (0.10ft/s), respectively, and this six-fold difference in velocity is due to the thermal plume above the head. With the fan OFF, the difference between velocity magnitudes at V1 (above the head) and at V2 (stagnation zone) was decreased, as shown in Figure 2. With the operation of the fan, a significant air mixing occurs and the buoyant thermal plume in the space is disturbed by the mixing flow. Figure 2 indicates that the duration of the transient period between the two operation modes (fan ON and fan OFF) is approximately one minute.

Thus, the operation of a fan operation affects airflow in the vicinity of a buoyant plume and in the entire space. When the fan operates, intensive air mixing occurs, disrupting the buoyant airflow. The experimental data demonstrate that the transition time between the two fan operation modes is relatively short (approximately 60 seconds) compared to fan operating or non-operating period. This result implies that, depending on the fan operation, the airflow in a residential building is primarily mixing flow or buoyant driven flow, not in a transition state between the two. The mixing and buoyant airflow patterns have different characteristics in air speed, turbulence intensity, and mixing intensity. Accordingly, the two different airflow patterns could have distinct effects on the pollutant transport, dispersion and removal in the space. The following sections will examine pollutant distribution and occupant exposure associated with the two major airflow patterns in residence.

POLLUTANT TRANSPORT ASSOCIATED WITH RESIDENTIAL FAN OPERATION

The second part of the study investigated the effects of the residential fan operation on the transport of gaseous and particulate pollutants in three stages. First, experiments measured temporal and spatial concentrations of gaseous and particulate pollutants with a short-term point source release. Second, by using the mock-up test results, the study established and validated a CFD model to accurately predict the

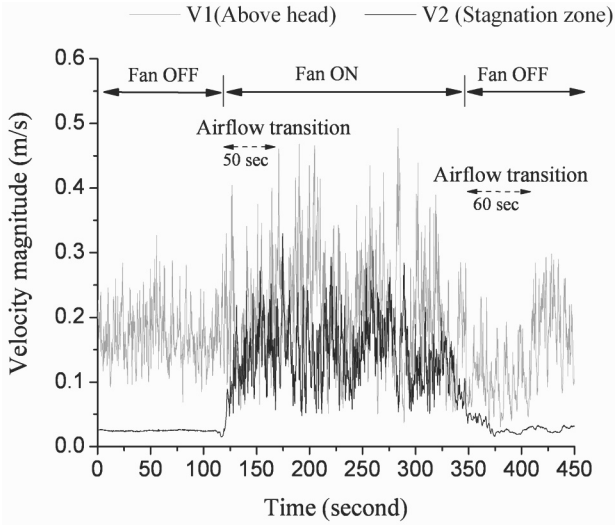

Figure 2 *Velocity magnitudes at two sampling points (above head and stagnation zone) with two fan operation modes: fan ON and fan OFF.*

transient pollutant concentrations. Third, the validated CFD model was further used to investigate spatial and temporal pollutant concentrations with the two characteristic airflow regimes: (1) mixing flow (fan ON) and (2) buoyancy driven flow (fan OFF).

Mock-Up Experiments to Validate CFD Model

The experiments with the buoyancy driven flow were used to develop high quality mock-up tests, given the challenges in modeling the varied level of turbulence with the buoyancy driven flow. Figure 3 shows a schematic diagram of the mock-up test including a 4.5 m x 5.5 m x 2.7 m (15' x 18' x 9') environmental chamber equipped with a thermal manikin, displacement diffuser, and indoor heat sources. The AHU of the environmental chamber controls the temperature and humidity of the inlet air, which was supplied at floor level using the displacement diffuser. The supplied air raised by heat sources in the space, generating buoyancy-induced airflow, and exhausted at the ceiling level. Heated boxes and a panel simulating indoor heat sources, such as computer and floor heating, were placed inside the chamber. The sampling apparatus included air velocity and temperature sensors, air sampling tubes, a tracer gas (SF_6) analyzer, and particle monitoring devices. To simulate transport of gaseous and particulate pollutants in residential buildings, SF_6 gas and three sizes of mono-disperse particles, respectively, were used.

In the experimental simulation of gaseous pollutant transport, low concentrations of a tracer gas (SF_6) were used to mimic real pollutants. Furthermore, the dynamics of three different sizes of particles, 0.03 μm, 1.5 μm, and 3.2 μm, with a density of 1.05 g/cm^3, were analyzed. The 0.03μm particles were used to represent ultrafine particles, which can cause respiratory and cardiovascular disease (Penttinen et al. 2002; Nemmar et al. 2002). The 1.5μm particles represent accumulation mode particles, such as those from tobacco smoke or incense. These particles have low deposition rates on indoor surfaces, air filters, and the upper respiratory region (Hind 1982; Nazaroff 2004). The 3.2 μm particles represent coarse mode particles, which have high settling velocities, compared to ultrafine particles or accumulation mode particles (Lai and Nazaroff 2000). These particles can be resuspended from indoor surfaces by human activity, such as walking or vacuum cleaning (Abt et al. 2000; Ferro et al. 2004; He et al. 2004).

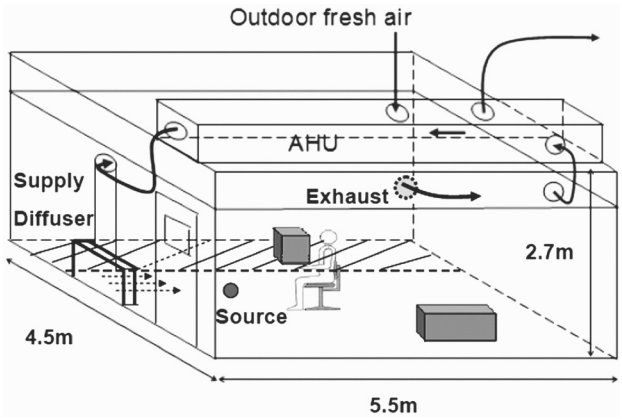

Figure 3 *Experimental setup for the mock-up tests, showing air handling unit, a manikin, heat sources, and a displacement diffuser.*

Four experiments were conducted to measure spatial and temporal concentrations of SF_6 gas and the three different-sized particles. During the experiment for gaseous pollutant transport, the SF_6 was injected at the source position, as shown in Figure 3, for a twelve-minute period and monitored for one hour. An SF_6 analyzer (Gas Chromatograph/Electron Capture Detector) collected and analyzed air samples from two different positions in the space: (1) the location 25 cm (9.8 in) above manikin head and (2) the location 120 cm (47.2 in) above the heated box on the floor. Similarly, during the experiments for particle transport, the three sizes of particles were released at a constant rate for a two-minute-period at the source location and monitored for an hour. The particles were injected into the space using a collision nebulizer. To monitor particle concentration, two particle monitoring devices were used: an ultrafine particle counter (P-Trak) and Aerotrak optical particle counter. The P-Trak monitored the concentration of 0.03 μm particles while The Aerotrak optical particle counter measured concentrations of 1.5μm and 3.2 μm particles.

Validation of CFD Model for Unsteady-State Pollutant Flow Analysis

For the numerical analyses of gaseous and particulate pollutant transport the CFD software FLUENT (2006) was used. Large efforts were dedicated to validation of the applied numerical models to assure the quality of data produced in these simulations. Based on the recommendations provided in previous CFD validation studies (Chen and Srebric 2002; Sørensen and Neilsen 2003), the parameters in the CFD model, which include the computational grid, turbulence model, boundary conditions, near-wall treatment, calculation time step and number of particles, were adjusted to establish a reliable CFD model. The results from the CFD model and previously described mock-up experiments were compared in the following order: temperature and velocity field, SF_6 concentration, and particle concentrations.

CFD Validation: Temperature & Velocity Field

In the tests for validation of the applied CFD models, the model geometry was identical to that of the experimental mock-up test. The only difference is in the geometry of the manikin. The detailed manikin geometry affects the airflow only in the vicinity of the manikin and does not affect the overall airflow in the space (Topp et al. 2002). Because the present study examined the overall airflow and pollutant transport in the space, simple rectangular geometry was used for the manikin.

To simulate turbulent eddies associated with buoyancy driven flow, the RNG k-ε model was applied as a turbulent

model. The application of the RNG k-ε model was based on previous studies (Chen 1995; Posner et al. 2003), which reported that the RNG *k*-ε turbulence model best predicts the turbulent indoor airflow among two-equation turbulence models. To assure the accuracy of the CFD model, the temperature and airflow fields calculated from CFD were compared with the experimental data. The validation showed that the CFD model calculates the temperature field with an accuracy of 0.5 °C (0.9 °F). Figure 4 shows the velocity profile at three monitoring locations in the room. Velocity magnitudes at V3 and V4 (ambient region) calculated from the CFD model were in good agreement with the experimental data. The only discrepancy between the experimental and simulation results is for the velocity profiles at V5 (close to the manikin), as shown in Figure 4d, which is likely due to the simplified geometry of the thermal manikin, and it does not affect the overall distribution in the room.

CFD Validation: SF_6 Concentration

During the SF_6 validation experiments, air samples were collected and monitored at the exhaust and two sampling points every six minutes for an hour. In the CFD simulation, a calculation time step of six seconds and a monitoring time step of one minute were used. To assure the quality of the experimental data and CFD results, the SF_6 concentration at the exhaust was compared to the analytical solution for a perfect-mixing flow condition, which is a transient mass balance on SF_6 gas yielding following relationship.
Injection period:

$$\left(C(t) = \frac{E}{Q}(1 - e^{-\lambda t}),\ 0 \le t \le 12\ \text{min}\right)$$

Decaying period:

$$C(t) = C(t \equiv 12\ \text{min})e^{-\lambda(t-12)},\ 12\ \text{min} < t \le 60\ \text{min}$$

where $C(t)$ is the SF_6 concentration, E is the SF_6 emission rate, Q is the volume flow rate, and λ is the air exchange rate.

Figure 5 displays the SF_6 concentrations from experiments and CFD simulation. The analytical solution of temporal change of SF_6 concentrations for perfect mixing exists only for the exhaust position, and Figure 5b compares the analytical, experimental, and numerical results. This figure shows that range of accuracy for the CFD results is similar to that of the experimental results. Figure 5c indicates that the CFD model reasonably predicts the peak concentration and time to the peak for sampling position S1, given that the CFD results track the general pattern of the measured SF_6 concentration. Figure 5d shows that at sampling position S2, CFD results and measurements agree well in the time of peak concentration with some difference in peak value. Considering these validation results, the developed CFD model proves to be capable of predicting the transient gaseous concentration with an acceptable accuracy.

CFD Validation: Particle Concentration

To validate the particle transport model, the spatial and temporal particle concentrations in the chamber were modeled for three different sizes of particles: 0.03 μm, 1.5 μm, and 3.2 μm. Using Lagrangian particle modeling, the trajectory of each particle was determined using the particle momentum equation (Zhang and Chen 2006), which equates particle inertia with four external forces acting on the particles: drag, lift, thermophoretic forces, and Brownian motion. Special attention was dedicated to the particle dynamics in the vicinity of the surfaces, as follows. When striking a rigid wall, particles either attach to or rebound from the wall surface. Lai and Nazaroff (2000) showed that the particle deposition rate is approximately two orders of magnitude larger for the floor surface than for vertical or ceiling surfaces. Therefore, in this study, a trap boundary condition was applied to the floor, whereas rebound condition was used for the wall and ceiling surfaces.

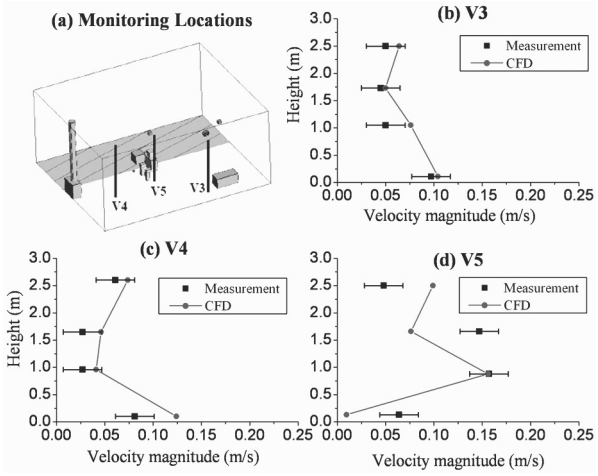

Figure 4 *Validation results: Velocity magnitudes from CFD and experiments at the monitoring locations.*

The mean path of the particle was calculated using a time-averaged flow field. The turbulent dispersion of the particle from the mean path was modeled by applying a stochastic particle tracking method, which determines the particle trajectory based on instantaneous fluctuating flow velocity. Given the stochastic nature of particle tracking, the stability of the calculation was evaluated based on particle tracking time steps, number of grids, and injected number of particles.

Sensitivity analysis of the time step for particle tracking and CFD was used to provide solutions independent of the size of the time step. Grid dependence was also checked by comparing the flow velocity and concentration distribution with measurements. A total grid number of approximately 100,000 was found to be appropriate to produce reasonable simulation results. Furthermore, to get a statistically significant number of particle samples in the monitoring regions S1 and S2 defined in Figure 5a, the total number of necessary particles was calculated to be 700,000. This number is several orders of magnitude less than the number of particles injected in the experiments, and for comparison of experimental and CFD results, particle concentrations were normalized by the time-integrated total number of particles measured or calculated at the two sampling locations. Using this normalization, the results from CFD modeling and experimental results are directly comparable as shown in Figure 6.

Figure 6 presents transient concentrations for the three investigated sizes of particles. It shows that for the given flow and space geometry, the peak particle concentrations occur several minutes after injection. Furthermore, the time to reach the peak concentration varies with sampling location and particle size. The peak concentrations represent temporal changes in the particle concentration, while the concentration difference between the two sampling locations (S1, S2) reflects the spatial distribution of particles in buoyant airflow. The results show that, for the developed CFD model, the calculated particle concentrations agree well with the measured data. Even though CFD results do not perfectly match the measurement data, CFD predicts temporal variation and peak concentration of particles with reasonable accuracy. The differences in time and peak concentration between CFD and measurements may be due to the simplified manikin geometry or due to the turbulent flow in the vicinity of the thermal plume. However, similar particle concentration patterns obtained from the CFD model and measurements suggest that the CFD model is accurate enough to provide insight into transient dispersion of particles in rooms with different airflow patterns.

PREDICTION OF POLLUTANT DISTRIBUTION USING VALIDATED NUMERICAL MODEL

Mixing Flow vs. Buoyant Flow

The validated CFD model was further used to investigate the spatial and temporal pollutant concentrations with and without the fan operating. This section presents the simulation results of transient gaseous and particulate contaminant transport under two airflow regimes: (1) momentum driven mixing flow and (2) buoyancy driven flow.

The momentum of the air supply jets creates air mixing typical for a residential space with air-conditioning, whereas the low velocity air supply from the displacement ventilation diffuser represents a naturally ventilated space in which buoy-

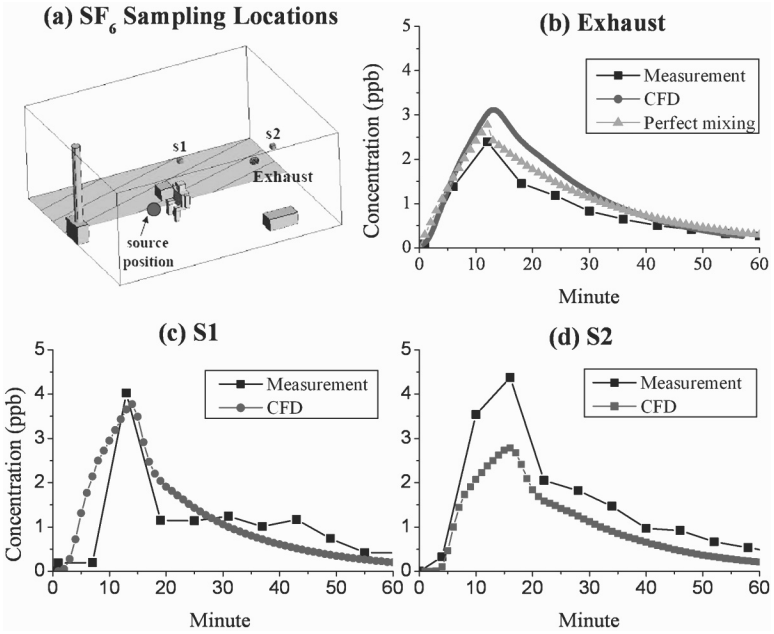

Figure 5 *Validation results: SF_6 concentrations at the exhaust and two sampling positions.*

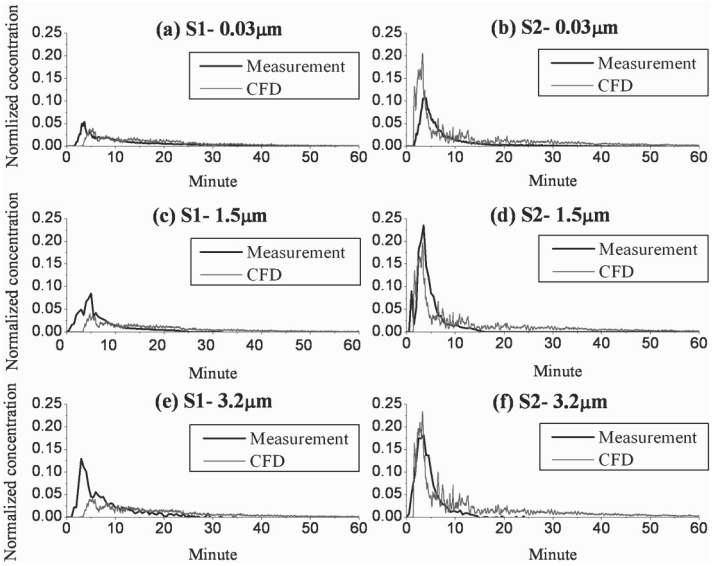

Figure 6 *Validation results: Concentrations of 0.03 μm, 1.5 μm, and 3.2 μm particles at the two sampling locations with an initial two-minute point-source release in the buoyancy driven flow regime. The air exchange rate was 2.7 hr^{-1}.*

ant airflow is dominant. Figure 7 shows the geometries of the numerical models used to simulate the mixing flow and buoyant flow, in a room with an air exchange rate of 2.7 hr^{-1}. In both cases, SF_6 gas and particles were steadily injected for two minutes and monitored for an hour at two characteristic sampling positions S1 and S2, located above the manikin's head and above the heated box, respectively. The pollutant concentrations monitored at the two sampling positions illustrate characteristics of occupant exposure and pollutant transport in the vicinity of the heat source.

Figure 8 presents the simulation results for the concentrations of SF_6 and particles at sampling points S1 and S2 in the two flow regimes. The modeled concentrations at the sampling points are also compared to the analytical solution for perfect mixing in the room. Figures 8a and 8b show that the SF_6 concentrations are two to five times higher with buoyant flow than with mixing flow, at both S1 and S2. With mixing flow, regardless of the sampling location, the concentration profiles at both sampling positions are almost identical, suggesting little spatial variation of SF_6 concentration in the mixing airflow. However, with buoyant flow, the temporal and spatial variation of SF_6 concentration is larger than the mixing flow, as shown in Figure 8b. The SF_6 results also indicate that the SF_6 concentrations in the mixing flow (Figure 8a) similarly match the perfect mixing concentration. However, the SF_6 concentrations sampled in the buoyant flow regime (Figure 8b) are up to five times higher than the perfect mixing concentration.

The non-uniform gaseous concentrations with buoyant flow in this stud y are in agreement with the previous study conducted by Baughman et al. (1994). They measured high concentrations of gaseous pollutants in a room with natural convection and found that indoor air quality model based on complete air mixing is not appropriate for short-term exposure in a buoyant flow. The results from the present study and Baughman et al. (1994) suggest that it is likely invalid to use the well-mixed assumption to accurately predict the level of occupant exposure in buoyant flow.

Similar to the SF_6 results, the particle simulation data presented in Figure 8 indicate lower levels of particle concentrations with mixing flow than with buoyant flow, little spatial variation of concentration in a mixing flow, and large temporal and spatial variation in a buoyant flow. With regards to the particles, the difference in the peak concentration between mixing flow and buoyant flow is apparent. The comparison of the particle concentrations in mixing flow and buoyant flow indicate that particle concentrations with the buoyancy driven flow can be up to thirty times higher than that with the mixing flow. These higher particle concentrations are likely due to the local heat sources which strongly drive the airflow and particles at the floor level to the upper region. This result implies that the level of exposure in the vicinity of heat sources, including occupants, can be much higher than in the bulk air region.

The results in Figure 8 show only very minimal differences in concentration pattern among different sizes of particles. The similar concentration patterns for different sizes of particles may be explained by the fact that for the analyzed air flow rate the time scale of particle deposition from diffusion and settling is longer than mean particle residence time in the space. Consequently, most of the particles in the space are likely to be either suspended in the room air or exhausted to the outdoors. In this study, the sampling location is far from the surface boundary layer and thus the transient particle concentration pattern seems to depend greatly on the overall airflow pattern in the bulk air region.

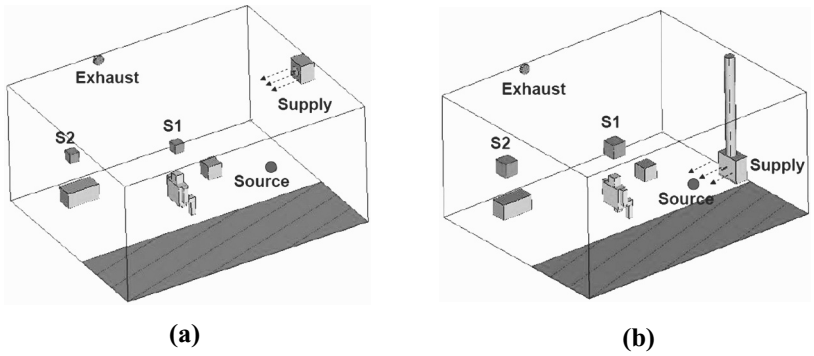

Figure 7 *Geometry of models used to simulate momentum driven mixing flow (a) and buoyancy driven flow (b).*

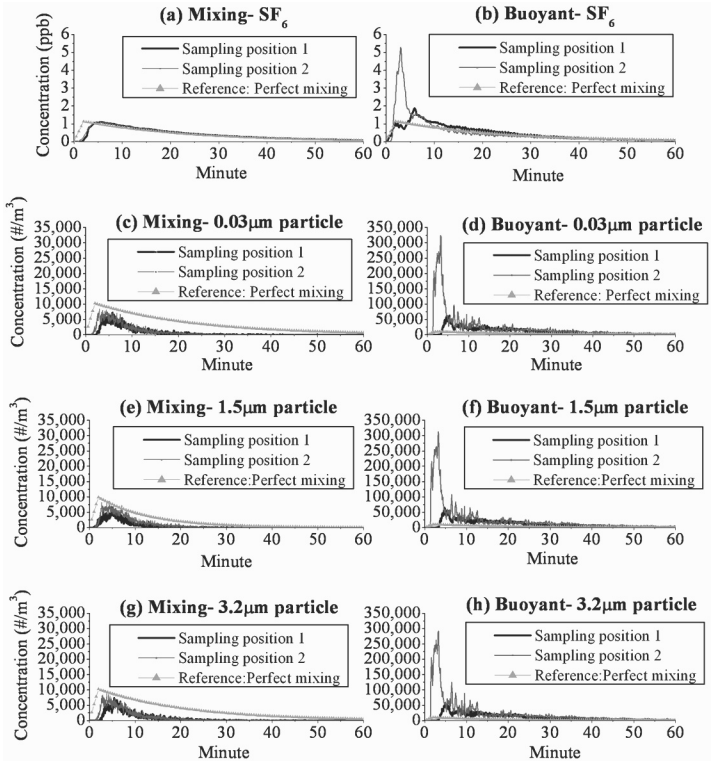

Figure 8 *Transient concentrations of SF_6, 0.03 μm, 1.5 μm, and 3.2 μm particles at the two sampling locations with mixing flow and buoyant flow. For both cases, the source release period was two minutes. The air exchange rate was 2.7 hr^{-1}. Note that the vertical scale for particles is ten times larger in the graphs for buoyant flow than those for mixing flow.*

Figure 8 also compares the particle concentrations obtained with the analytical solution for perfect mixing to those from the numerical modeling results. The perfect mixing particle concentrations were produced by using a mass balance with size-dependent deposition loss rates summarized by Riley et al. (2002).

Figures 8c, 8e and 8g show relatively uniform concentrations with mixing flow. At sampling positions S1 and S2, the shape of the temporal concentration distribution obtained by CFD particle tracking model is similar to the perfect mixing concentration pattern obtained by the analytical solution using Equation 1; the difference is only in the lower peak concentration and faster decay rate for results obtained by the CFD simulations. This difference is most likely caused by the short period of injection (two minutes) with respect to the mixing time (the air exchange rate was 2.7 hr^{-1}) and the position of the source relative to the sampling positions. In the case of buoyant flow (Figures 8d, 8f, and 8h), the particle concentrations are one to two orders of magnitudes higher than the perfect mixing concentration. This highly non-uniform concentration likely occurs when locally developed airflow near the heat sources transports the particles into the vicinity of the charac-

teristic sampling locations. Along with the spatial variation in the particle concentration, the temporal variation is an important characteristic of particle transport in a buoyant flow. The temporal variation in the particle concentrations between the two sampling locations is a consequence of the short-term point source release and the non-uniform distribution of local airflow in the buoyant flow regime.

Figure 8 Transient concentrations of SF_6, 0.03 μm, 1.5 μm, and 3.2 μm particles at the two sampling locations with mixing flow and buoyant flow. For both cases, the source release period was two minutes. The air exchange rate was 2.7 hr^{-1}. Note that the vertical scale for particles is ten times larger in the graphs for buoyant flow than those for mixing flow.

Table 1 summarizes a total exposure for the two sampling position over the period of one hour following the two-minute source activation. Table 1 indicates that the total exposures to the SF_6 gas and particles observed with buoyant flow are in a higher range than those with the mixing flow. For example, the total exposure to particles with buoyant flow is up to approximately fifty times higher than those with mixing flow. It seems that the high peak concentration of short-term pollutant source in buoyant flow (Figure 8) contributes to a high level of total exposure.

Table 1 also indicates that the spatial difference in total exposure between the two sampling positions is much larger with buoyant flow than mixing flow. For instance, with the buoyant flow, total exposures to particles at sampling position 2 are approximately thirty-forty times higher than those at sampling position 1. Note that the total exposure also depends on pollutant decay rate at the sampling position. Given the negligibly small difference in the decay rate between the two sampling positions, the spatial variation of the peak concentrations in the buoyant flow appears to play a crucial role in the spatial variation of the total exposure.

The results presented in Figure 8 and Table 1 complement previous studies related to pollutant distribution. Previous studies (Zhao et al. 2004; Zhang and Chen 2006; Gao and Niu 2007) examined particle transport mainly with a continuous particle emission from the source. Gao and Niu (2007) simulated particles with different airflow patterns and reported that the buoyant airflow associated with a local thermal plume can cause a high level of exposure to particles. However, based on the steady-state simulation results, they reported that buoyant airflow is preferable to mixing airflow in reducing exposure to fine particles. On the other hand, Zhao et al. (2004) conducted steady-state simulations to compare particle transport and deposition in mixing and buoyant airflow and reported larger average particle concentrations for the buoyant airflow. The present study simulated transient particle transport with a short-term point source release in the two airflow regimes and showed higher concentrations of particles ranging from 0.03 to 3.2 μm with buoyant flow than with mixing flow. This result implies that high exposure to short-time point release pollutants likely occur in residence when the buoyant flow is dominant, i.e., when ventilation fan is not operating.

To show the difference in concentration distribution with short-term and long-term sources, Figure 9 compares the peak SF_6 concentration with a short-term emission (two minutes) to the concentration with continuous (steady-state) emission. Comparison of concentrations at two locations presented in Figure 9 indicate that in a mixing flow, the difference in SF_6 concentration between two sampling locations is negligible for both transient and steady-state conditions. This pattern suggests that a well mixed condition is likely achieved for the mixing flow. However, with buoyant flow, the SF_6 peak concentration at S2 is approximately three times higher than that at S1, even though the steady-state concentration is almost the same. This result indicates that for the buoyant flow regime, the exposure to pollutants from a short-term source emission may not be consistent with the one from a steady-state source emission.The majority of indoor pollutants sources include cooking, walking, vacuuming and coughing, which are short-term release sources. Therefore, occupant exposure to a typical short-term indoor source may be different from the concentration estimated using the steady-state source emission. This result suggests cautions in drawing conclusions about occupant exposure in residence from steady-state emissions.

Table 1. Total Exposure to SF_6 Gas and Three Different-Sized Particles For One Hour After Source Activation

Total Exposure (Unit)	Mixing Flow		Buoyant Flow	
	Sampling Position 1	Sampling Position 2	Sampling Position 1	Sampling Position 2
SF_6 (ppb·min)	13.4	13.6	28.3	30.6
0.03 μm (#/m^3·min)	3,960	5,610	59,300	230,000
1.5 μm (#/m^3·min)	3,430	5,760	65,500	229,000
3.2 μm (#/m^3·min)	3,850	5,410	68,400	232,000

Mechanically Ventilated Space vs. Naturally Ventilated Space

The room air exchange rate is generally higher in a room with a fan operating than a room in which only natural convection airflow exists. This section of the present study examines pollutant transport in two typical residential rooms: a mechanically ventilated room with the mechanical fan ON and a naturally ventilated room with the fan OFF. The air exchange rates used for a mechanically ventilated room and a naturally ventilated room are 5 hr^{-1} and 0.5 hr^{-1}, respectively.

Figure 10 shows the resulting SF_6 and particle concentrations for the two analyzed rooms. The SF_6 concentration in the mechanically ventilated space is nearly uniform, implying intensive mixing of the air in the space. However, spatial and temporal variations in SF_6 concentration and slower decay rate (after the peak) exist in the naturally ventilated room. This is due to the non-uniform airflow distribution and low ventilation rate in the naturally ventilated room. The level of exposure to SF_6 gas is higher in the naturally ventilated room compared to the mechanically ventilated space. The particle concentration data show a concentration pattern similar to SF_6 results, including relatively uniform concentrations in the mechanically ventilated space, spatial and temporal variations in concentrations and high exposure in the naturally ventilated space. However, the variation in particle concentration is higher than that in SF_6 concentration. The peak particle concentration at S2 in the naturally ventilated space is up to thirty times higher than the one in the mechanically ventilated space, implying high potential of exposure to particles in the naturally ventilated space. These results suggest that acute exposure to transient pollutants can occur in a naturally ventilated space where the pollutant distribution is not uniform and local zones of high pollutant concentration exist.

The results in Figure 9 and 10 indicate higher risk for exposure to particulate pollutants with buoyant flow. However, it should be pointed out that the gaseous and particulate concentrations in a room depend on the source position. In this study, the source was located close to the floor and the effect of buoyant airflow on the pollutant concentration at the sampling position seemed to be very large. Further investigations with different source locations should be conducted to articulate the effect of indoor airflow pattern on the transient pollutant concentration pattern. Another limitation of this study is that the presented results consider airflow and contaminant distribution in a space assuming clean supply air. With air recirculation in air handling units, the recirculation rate influences the pollutant concentrations in the supply air. The effects of recirculation, including filtration and deposition of particles and reactions of gaseous pollutants in ventilation systems, have an important role in occupant exposure. Therefore, in an overall analysis of contaminant distribution in buildings, air recirculation should be taken into account. When the recirculated pollutant concentrations are known, the results presented in this study can be used to recalculate pollutant dispersion considering pollutant concentration in supply air.

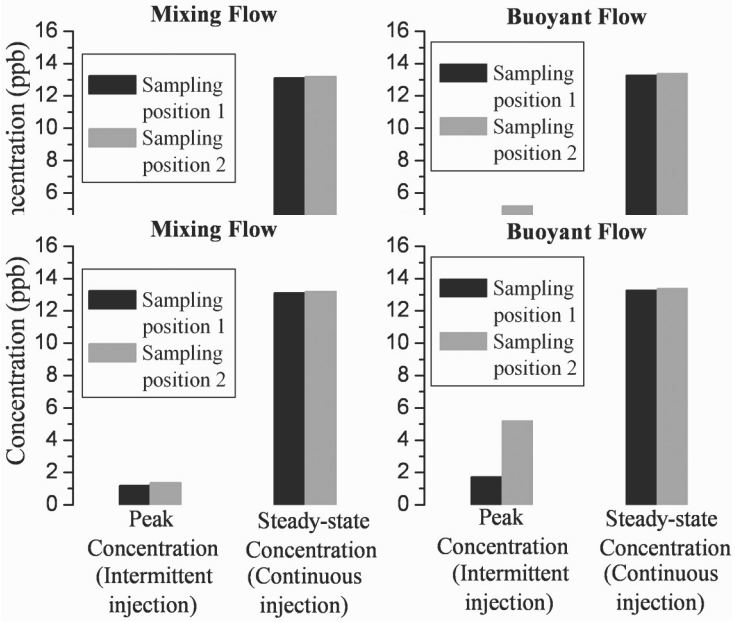

Figure 9 *Comparison between SF_6 peak (with intermittent injection) and steady-state (with continuous injection) concentrations at the two sampling locations with mixing flow and buoyant flow. For both cases, the air exchange rate was 2.7 hr^{-1}.*

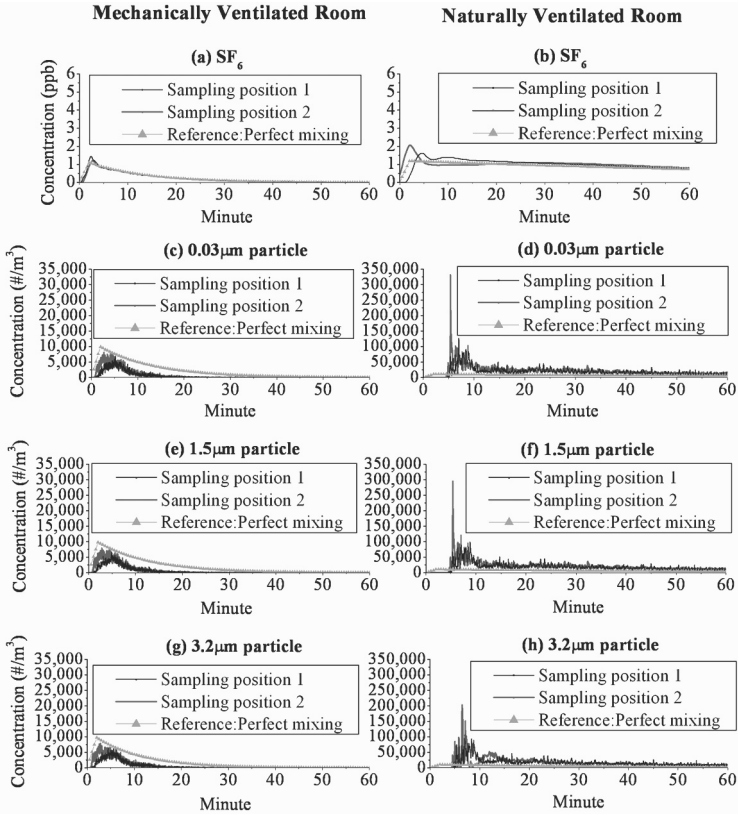

Figure 10 *Transient concentrations of SF_6, 0.03 μm, 1.5 μm, and 3.2 μm particles at the two sampling locations for two residential rooms: mechanically ventilated ($5hr^{-1}$) and naturally ventilated ($0.5hr^{-1}$) rooms. Note that the vertical scale for particles if ten times larger in the graphs for buoyant flow than those for mixing flow.*

CONCLUSION

In residential buildings, mechanical fans operate periodically, and the present study simulated the indoor airflow associated with periodic fan usage. The transition period between mixing flow (fan ON) and buoyant flow (fan OFF) was found to be approximately one minute, indicating that the airflow in residence is primarily either mixing flow or buoyant flow.

A CFD model and experiments were used to simulate short-term point source pollutant release in the two airflow regimes. The results show that the peak concentrations of gaseous and particulate pollutants can be much higher in a buoyant flow than in a mixing flow. The variation in particle concentration was higher than that in gaseous concentration. These results imply that a high level of exposure to short-term point release pollutants likely occurs in a residential room in which fan is not operating. The well-mixed assumption seems applicable in estimating the level of occupant exposure for mixing flow, but it is likely invalid to model exposure in a room with stratified flow. The comparison of the peak concentrations due to a transient source and a steady-state concentration with a continuous source suggests cautions in drawing conclusions about occupant exposure to a short-term indoor pollutant release from the steady-state release concentration, especially in a naturally ventilated space in which the mechanical fan is off.

The study results clearly demonstrate that using the well-mixed and steady-state assumptions to estimate the occupant exposure may not always be appropriate for a naturally ventilated residential space. Regarding the short-term exposure, future studies should assess the effect of source location on the exposure to pollutants.

ACKNOWLEDGMENTS

The research is partially supported by ASHRAE Grant-in-aid Fellowship and the National Science Foundation Integrative Graduate Education and Research Traineeship (IGERT) grant DCE-0549428, Indoor Environmental Science and Engineering, at The University of Texas at Austin. The authors are grateful for careful reviews of the manuscript by Catherine Mukai and Michael Waring.

REFERENCES

Abt, E., Suh, H.H., Catalano, P., and Koutrakis, P. 2000. Relative contribution of outdoor and indoor particle sources to indoor concentrations. Environmental science & technology 34 (17): 3579-3587.

Baughman, A.V., Gadgil, A.J., and Nazaroff, W.W. 1994. Mixing of a point-source pollutant by natural-convection flow within a room. Indoor air 4 (2): 114-122.

Bouilly, J., Limam, K., Beghein, C., and Allard, F. 2005. Effect of ventilation strategies on particle decay rates indoors: An experimental and modelling study. Atmospheric environment 39 (27): 4885-4892.

Chen, Q. 1995. Comparison of different k-? models for indoor air flow computations. Numerical heat transfer. Part B, Fundamentals, 28(3), 353-369.

Chen, Q. and Srebric, J. 2002. A procedure for verification, validation, and reporting of indoor environment CFD analyses, Int. J. HVAC & R Res.,8, 201–216.

FLUENT, 2006. Fluent 6.2 User's guide. Fluent Inc., Lebanon, NH.

Ferro, A.R., Kopperud, R.J., and Hildemann, L.M. 2004. Source strengths for indoor human activities that resuspend particulate matter. Environmental science & technology 38 (6): 1759-1764.

Gao, N.P., and Niu, J.L. 2007. Modeling particle dispersion and deposition in indoor environments. Atmospheric environment 41 (18): 3862-3876.

He, CR., Morawska, L.D., Hitchins, J., and Gilbert, D. 2004. Contribution from indoor sources to particle number and mass concentrations in residential houses. Atmospheric environment 38 (21): 3405-3415.

He, G., Yang, X., and Srebric, J. 2005. Removal of contaminants released from room surfaces by displacement and mixing ventilation: modeling and validation. Indoor air 15 (5): 367-380.

Hinds W.C. 1999. *Aerosol Technology*. New York: Wiley.

Huang, J.M., Chen, Q.Y., Ribot, B., and Rivoalen, H. 2004. Modelling contaminant exposure in a single-family house. Indoor and built environment 13 (1): 5-19.

Lai, A.C.K., and Nazaroff, WW. 2000. Modeling indoor particle deposition from turbulent flow onto smooth surfaces. Journal of aerosol science 31 (4): 463-476.

Li, Y., Leung, G.M., Tang, J.W., Yang, X., Chao, C.Y.H., Lin, J.Z., Lu, J.W., Nielsen, P.V., Niu, J., Qian, H., Sleigh, A.C., Su, H.J.J., Sundell, J., Wong, T.W., and Yuen, P.L. 2007. Role of ventilation in airborne transmission of infectious agents in the built environment - a multidisciplinary systematic review. Indoor air 17(1): 2-18.

Lin, Z., Chow, T.T., Fong, K.F., Tsang, C.F., and Wang, Q.W. 2005. Comparison of performances of displacement and mixing ventilations. Part II: indoor air quality. Revue internationale du froid, 28(2): 288-305.

Murakami, S., Kato, S., Zeng, J. 1997. Flow and temperature fields around the human body with various room air distribution, CFD study on computational thermal manikin – Part I. *ASHRAE Transactions* 103:3-15

Nazaroff, WW. 2004. Indoor particle dynamics. Indoor air 14: 175-183.

Nemmar, A., Hoet, P.H.M., Vanquickenborne, B., Dinsdale, D., Thomeer, M., Hoylaerts, M.F., Vanbilloen, H., Mortelmans, L., and Nemery, B. 2002. Passage of inhaled particles into the blood circulation in humans. Circulation 105 (4): 411-414.

Novoselac, A., and Srebic, J. 2002. A critical review on the performance and design of combined cooled ceiling and displacement ventilation systems. Energy and buildings 34 (5): 497-509.

Penttinen, P., Timonen, K.L., Tiittanen, P., Mirme, A., Ruuskanen, J., and Pekkanen, J. 2001. Ultrafine particles in urban air and respiratory health among adult asthmatics. The European respiratory journal 17 (3): 428-435.

Posner, J.D., Buchanan, C.R., and Dunn-Rankin, D. 2003. Measurement and prediction of indoor air flow in a model room. Energy and buildings 35 (5): 515-526.

Riley, W.J., McKone, K.E., Lai, A.C.K., and Nazaroff, W.W. 2002. Indoor particulate matter of outdoor origin: Importance of size-dependent removal mechanisms. Environmental science & technology 36 (2): 200-207.

Sørensen, D.N., and Neilsen, P.V. 2003. Quality control of computational fluid dynamics in indoor environments. Indoor air 13 (1): 2-17.

Topp, C., Nielsen, P.V. and Sørensen, D.N. 2002. Application of Computer Simulated Persons in Indoor Environmental Modeling. ASHRAE Transactions, 108 (2), p. 1084-1089.

Ward, M., Siegel, J.A., and Corsi, R.L. 2005. The effectiveness of stand alone air cleaners for shelter-in-place. Indoor air 15 (2): 127-134.

Zhang, Z., and Chen, Q. 2006. Experimental measurements and numerical simulations of particle transport and distribution in ventilated rooms. Atmospheric environment 40 (18): 3396-3408.

Zhao, B., Li, X.T., and Zhang, Z. 2004. Numerical study of particle deposition in two differently ventilated rooms. Indoor and built environment 13 (6): 443-451.

DISCUSSION

H. Ezzat Khalifa, Professor, Syracuse University, Syracuse, NY: There was a paper by Sideroff et al. in Transactions Session 2 yesterday in which a very detailed representation of the manikin and its microenvironment was included in several CFD simulations with k-ε, Vzf, and LES models. The results were compared with experimental data obtained by Professors Nielsen and Katz. Sideroff showed little advantage of LES over k-ε with each wall treatment. He found the inclusion of radiation in CFD is far more important.

Donghyun Rim: We agree with Professor Khalifa's comment, and that is the reason we used k-ε turbulence model in our simulations. Also, in our CFD models we took into account effects of radiation by calculating convective and radiative portions of heat fluxes at surfaces based on experimental results. By using only the convective portion of the total heat flux for Neumann boundary conditions, we secured accuracy of thermal boundary conditions in our CFD and particle tracking models.

Paul Lebbin, Mechanical Engineer, J.L. Richards & Associates, North Bay, ON, Canada: Very interesting results

between measured and predicted CFD results. I would have liked a detailed description of the measurement equipment to see how the particles are released/measured. As you know, this is criteria in CFD verification.

Donghyun Rim: In our validation experiments, we used latex monodispersed particles with a density of 1.05 g/cm^3. Separate experiments were conducted for 0.03, 1.5, and 3.2 μm particles. The particles were seeded with a constant rate at the source position using the Collison Nebulizer. The particle injection created a several-order higher particle concentration in the space than the initial (background) concentration. This way, we eliminated inaccuracy in measurement caused by the background concentration. We monitored spatial and temporal distribution of 0.03 μm particles using condensation particle counters (CPC), and for 1.5 and 3.2 μm particles we used optical particle counters (OPC). All of the instruments used in our study were calibrated before the measurements.